Re-entrant corner flows of UCM fluids: The natural stress basis

J.D. Evans*
Department of Mathematical Sciences, University of Bath,
Bath BA2 7AY, United Kingdom

April 28, 2006

Abstract

This paper continues the description of a two parameter family of solutions for the local asymptotic behaviour of UCM fluids at re-entrant corners. Here, the natural stress basis is used to re-derive the equations in the core flow and boundary layers, with full description of the scalings and matching being given. The parametric solution dependence is completed with numerical deteremination of the coefficient of the downstream wall shear rate. The flow structure implicitly assumes the absence of a separating streamline in the upstream region.

Key words and phrases: UCM fluid; re-entrant corner; boundary layer; self-similar solutions; natural stress basis

* e-mail: masjde@maths.bath.ac.uk

1. Introduction

Description of the local asymptotic solution for flow of UCM fluids around sharp corners, continues here with its formulation using the natural stress basis. The development parallels that of the first paper [1] with the core flow (outer region) and wall boundary layers (inner regions) being identified and analyzed separately.

The layout of the paper is as follows. In the rest of this introduction we record the main mathematical results relating to the natural stress basis that will be extensively used in the susbsequent analysis. The outer solution is addressed in section 2, whilst the boundary layer equtions are analyzed in section 3. The parametric solution description is then addressed in section 4 where the upstream and downstream boundary layers are considered separately. Numerical solution of the downstream layer is addressed, with the determination of the downstream wall shear rate.

We are considering steady planar flow of UCM fluids around a sharp corner, the dimensionless governing equations, geometry and local asymptotic structure for which has been described in [1]. We are considering the case We $=1$ without loss of generality and make the following preliminary remarks to introduce the natural stress basis and record important previously obtained results.

Remark 1: Cartesian formulation. The momentum and consitutive equations can be written in the form

$$\mathrm{Re}\,\mathbf{v}\cdot\nabla u = -\frac{\partial p}{\partial x} + \frac{\partial T_{11}}{\partial x} + \frac{\partial T_{12}}{\partial y}, \tag{1.1}$$

$$\mathrm{Re}\,\mathbf{v}\cdot\nabla v = -\frac{\partial p}{\partial y} + \frac{\partial T_{12}}{\partial x} + \frac{\partial T_{22}}{\partial y}, \tag{1.2}$$

and

$$T_{11} + \left(u\frac{\partial T_{11}}{\partial x} + v\frac{\partial T_{11}}{\partial y} - 2\frac{\partial u}{\partial y}T_{12} - 2\frac{\partial u}{\partial x}T_{11}\right) = 2\frac{\partial u}{\partial x}, \tag{1.3}$$

$$T_{22} + \left(u\frac{\partial T_{22}}{\partial x} + v\frac{\partial T_{22}}{\partial y} - 2\frac{\partial v}{\partial x}T_{12} - 2\frac{\partial v}{\partial y}T_{22}\right) = 2\frac{\partial v}{\partial y}, \tag{1.4}$$

$$T_{12} + \left(u\frac{\partial T_{12}}{\partial x} + v\frac{\partial T_{12}}{\partial y} - \frac{\partial v}{\partial x}T_{11} - \frac{\partial u}{\partial y}T_{22}\right) = \frac{\partial u}{\partial y} + \frac{\partial v}{\partial x}. \tag{1.5}$$

The velocity field is

$$\mathbf{v} = (u, v) = \left(\frac{\partial \psi}{\partial y}, -\frac{\partial \psi}{\partial x}\right), \tag{1.6}$$

where ψ is the stream function.

Remark 2: Natural stress basis. It is convenient to express the stress tensor with respect to a natural stress basis spanned by the velocity field and its orthogonal counterpart as described by Renardy [4], [7]. Specifically, we introduce the vector $\mathbf{w}$ given by

$$\mathbf{w} = (w_1, w_2) = \left(-\frac{v}{u^2+v^2}, \frac{u}{u^2+v^2}\right)$$

orthogonal to $\mathbf{v}$ and satisfying $|\mathbf{v} \times \mathbf{w}| = 1$. Then $\mathbf{T}$ can be represented in a basis formed with the dyadic products of $\mathbf{v}$ and $\mathbf{w}$, namely

$$\mathbf{T} = -\mathbf{I} + \lambda \mathbf{v}\mathbf{v}^T + \mu(\mathbf{v}\mathbf{w}^T + \mathbf{w}\mathbf{v}^T) + \nu \mathbf{w}\mathbf{w}^T.$$

The components of the Cartesian and natural stress bases are related as follows

$$\begin{aligned} T_{11} &= -1 + \lambda u^2 - \frac{2\mu uv}{(u^2+v^2)} + \frac{\nu v^2}{(u^2+v^2)^2}, \\ T_{12} &= \lambda uv + \frac{\mu(u^2-v^2)}{(u^2+v^2)} - \frac{\nu uv}{(u^2+v^2)^2}, \\ T_{22} &= -1 + \lambda v^2 + \frac{2\mu uv}{(u^2+v^2)} + \frac{\nu u^2}{(u^2+v^2)^2}. \end{aligned} \tag{1.7}$$

Here $\lambda(x,y), \mu(x,y)$ and $\nu(x,y)$ are variables now aligned along streamlines and we note that

$$\det(\mathbf{T}+\mathbf{I}) = \lambda\nu - \mu^2. \tag{1.8}$$

Correspondingly, (1.3)–(1.5) become

$$\lambda + \mathbf{v}\cdot\nabla\lambda + 2\mu\nabla\cdot\mathbf{w} = \frac{1}{u^2+v^2}, \qquad \mu + \mathbf{v}\cdot\nabla\mu + \nu\nabla\cdot\mathbf{w} = 0, \qquad \nu + \mathbf{v}\cdot\nabla\nu = u^2+v^2, \tag{1.9}$$

where

$$\nabla\cdot\mathbf{w} = \frac{1}{(u^2+v^2)^2}\left((v^2-u^2)\left(\frac{\partial v}{\partial x} + \frac{\partial u}{\partial y}\right) + 4uv\frac{\partial u}{\partial x}\right),$$

whilst the momentum equations (1.1)–(1.2) become

$$\mathrm{Re}\,\mathbf{v}\cdot\nabla u = -\frac{\partial p}{\partial x} + \mathbf{v}\cdot\nabla(\lambda u) + \nabla\cdot\left(\mu u\mathbf{w} - (\mu\mathbf{v} + \nu\mathbf{w})\frac{v}{(u^2+v^2)}\right), \tag{1.10}$$

$$\mathrm{Re}\,\mathbf{v}\cdot\nabla v = -\frac{\partial p}{\partial y} + \mathbf{v}\cdot\nabla(\lambda v) + \nabla\cdot\left(\mu v\mathbf{w} + (\mu\mathbf{v} + \nu\mathbf{w})\frac{u}{(u^2+v^2)}\right). \tag{1.11}$$

Remark 3: Wall boundary layers. Analogous to remark 3 in the introduction in [1], the same equations are assumed to hold near both the upstream and downstream walls. If Cartesian axes are taken to be aligned with the upstream wall, then the downstream layer can then be considered by allowing for a change in the flow direction and re-orientation of the axes by the transformation

$$\psi \mapsto -\psi, \qquad y \mapsto -y, \qquad \mu \mapsto -\mu, \tag{1.12}$$

the other variables being unchanged. This transformation leaves the governing equations invariant and relative to the upstream layer, its net effect is to simply change the sign of the stream function and the natural stress variable μ when considering the downstream layer.

Remark 4: The leading order outer solution. In the outer (core) region, we have Hinch's [2] leading order solution

$$\psi = c_0 r^{\alpha n}\sin^n(\alpha\theta), \qquad \mathbf{T} = \lambda(\psi)\,\mathbf{v}\mathbf{v}^T \qquad \text{as } r \to 0, \tag{1.13}$$

with

$$\lambda(\psi) = c_1\left(\frac{\psi}{c_0\alpha^n}\right)^{\frac{2}{n}-2},$$

where c_0, c_1 are arbitrary constants and the index n is given by

$$n = 3 - \alpha. \tag{1.14}$$

Remark 5: The approximation of $\mathbf{T}+\mathbf{I}$ by a rank one tensor. In [1] we have shown that

$$\det(\mathbf{T}+\mathbf{I}) = \Delta_0 \left(\frac{\psi}{c_0\alpha^n}\right)^{-\frac{2(1-\alpha)}{n}} \tag{1.15}$$

holds at leading order in the core outer region. The strictly positive constant Δ_0 was determined by matching to the upstream boundary layer. This observation can be used to determine the scalings for the natural stress variables μ and ν in the core outer region. We previously remarked that since $\mathbf{T}+\mathbf{I}$ is a rank one tensor at leading order, the governing equations in general satisfy a form of the compressible Euler equations as described by Renardy [7]. However, since λ, μ and ν are not the same sizes it is worth noting that we actually obtain the incompressible form of the Euler equations for the flow and stress fields associated with the similarity solution (1.13).

2. The outer core region

Following the scalings

$$r = \epsilon R^*, \quad x = \epsilon X^*, \quad y = \epsilon Y^*, \quad \psi = \epsilon^{n\alpha}\Psi^*, \quad \mathbf{T} = \epsilon^{-2(1-\alpha)}\mathbf{T}^*, \quad p = \epsilon^{-2(1-\alpha)}p^*, \tag{2.1}$$

from [1] with $0 < \epsilon \ll 1$, we introduce

$$\mathbf{v} = \epsilon^{n\alpha-1}\mathbf{v}^*, \quad \mathbf{w} = \epsilon^{1-n\alpha}\mathbf{w}^*, \quad \lambda = \epsilon^{-2\alpha(n-1)}\lambda^*, \quad \mu = \epsilon^{\alpha(\alpha-1)}\mu^*, \quad \nu = \epsilon^{2\alpha}\nu^*, \tag{2.2}$$

where the scaling for λ follows from the solution (1.13) and the scalings for μ and ν may be deduced from (1.8) and (1.15) when written in outer variables. More directly, the scalings for μ and ν can be obtained by matching to their values in the upstream boundary layer, this information already being contained in (1.15). In outer variables, the momentum equations (1.10)–(1.11) become

$$\begin{aligned}
\mathrm{Re}\,\epsilon^{2\alpha(2-\alpha)}\,\mathbf{v}^*\cdot\nabla^*u^* = {} & -\frac{\partial p^*}{\partial x^*} + \mathbf{v}^*\cdot\nabla^*(\lambda^*u^*) + \delta\nabla^*\cdot\left(\mu^*u^*\mathbf{w}^* - \mu^*\mathbf{v}^*\frac{v^*}{(u^{*2}+v^{*2})}\right) \\
& + \delta^2\nabla^*\cdot\left(\nu^*\mathbf{w}^*\frac{v^*}{(u^{*2}+v^{*2})}\right), \qquad (2.3) \\
\mathrm{Re}\,\epsilon^{2\alpha(2-\alpha)}\,\mathbf{v}^*\cdot\nabla^*v^* = {} & -\frac{\partial p^*}{\partial y^*} + \mathbf{v}^*\cdot\nabla^*(\lambda^*v^*) + \delta\nabla^*\cdot\left(\mu^*v^*\mathbf{w}^* + \mu^*\mathbf{v}^*\frac{u^*}{(u^{*2}+v^{*2})}\right) \\
& + \delta^2\nabla^*\cdot\left(\nu^*\mathbf{w}^*\frac{u^*}{(u^{*2}+v^{*2})}\right). \qquad (2.4)
\end{aligned}$$

and the constitutive equations (1.9)

$$\begin{aligned}
& \mathbf{v}^*\cdot\nabla^*\lambda^* + \delta\left(2\mu^*\nabla^*\cdot\mathbf{w}^* + \lambda^*\right) = \epsilon^{(4-\alpha)(1-\alpha)}(u^{*2}+v^{*2})^{-1}, \\
& \mathbf{v}^*\cdot\nabla^*\mu^* + \delta\left(\nu^*\nabla^*\cdot\mathbf{w}^* + \mu^*\right) = 0, \\
& \mathbf{v}^*\cdot\nabla^*\nu^* + \delta\nu^* = \epsilon^{\alpha(1-\alpha)}(u^{*2}+v^{*2}), \qquad (2.5)
\end{aligned}$$

where we introduce for convenience the gauge

$$\delta = \epsilon^{2-n\alpha} = \epsilon^{(1-\alpha)(2-\alpha)}.$$

The expressions (1.7) become

$$\begin{aligned} T_{11}^* &= -\epsilon^{2(1-\alpha)} + \lambda^* u^{*2} - \delta \frac{2\mu^* u^* v^*}{(u^{*2}+v^{*2})} + \delta^2 \frac{\nu^* v^{*2}}{(u^{*2}+v^{*2})^2}, \\ T_{12}^* &= \lambda^* u^* v^* + \delta \frac{\mu^*(u^{*2}-v^{*2})}{(u^{*2}+v^{*2})} - \delta^2 \frac{\nu^* u^* v^*}{(u^{*2}+v^{*2})^2}, \\ T_{22}^* &= -\epsilon^{2(1-\alpha)} + \lambda^* v^{*2} + \delta \frac{2\mu^* u^* v^*}{(u^{*2}+v^{*2})} + \delta^2 \frac{\nu^* u^{*2}}{(u^{*2}+v^{*2})^2}, \end{aligned} \tag{2.6}$$

Posing

$$\begin{gathered} \Psi^* = \Psi^{*(0)} + o(1), \quad \mathbf{T}^* = \mathbf{T}^{*(0)} + o(1), \quad p^* = p^{*(0)} + o(1), \\ \lambda^* = \lambda^{*(0)} + o(1), \;\; \mu^* = \mu^{*(0)} + o(1), \;\; \nu^* = \nu^{*(0)} + o(1), \qquad \text{as } \epsilon \to 0, \end{gathered} \tag{2.7}$$

we have from (2.5) that $\lambda^{*(0)}, \mu^{*(0)}, \nu^{*(0)}$ are functions of $\Psi^{*(0)}$. We make the specific assumptions that these dependencies are of power law form, namely

$$\lambda^{*(0)} = d_1 \left(\frac{\Psi^{*(0)}}{c_0 \alpha^n}\right)^{n_1}, \quad \mu^{*(0)} = d_2 \left(\frac{\Psi^{*(0)}}{c_0 \alpha^n}\right)^{n_2}, \quad \nu^{*(0)} = d_3 \left(\frac{\Psi^{*(0)}}{c_0 \alpha^n}\right)^{n_3}, \tag{2.8}$$

for arbitrary constants d_1, d_2, d_3, c_0 and exponents n_1, n_2, n_3, n. Here we have conveniently introduced the constant c_0, which will be defined below, to avoid using modulus signs. The important observation is that the leading order natural stress variables are constant on leading order streamlines, the information that they contain being carried unchanged through the core outer region. The values these variables receive from the upstream layer are then delivered to the downstream layer, these variables linking the information for the two boundary layers together. Following [5] and [7], the momentum equations give

$$0 = -\nabla^* p^{(0)} + \mathbf{v}^{*(0)} \cdot \nabla^* (\lambda^{*(0)} \mathbf{v}^{*(0)}),$$

which, on introducing

$$\mathbf{u} = (\lambda^{*(0)})^{\frac{1}{2}} \mathbf{v}^{*(0)} \tag{2.9}$$

gives the steady incompressible Euler equations

$$\nabla^* \cdot \mathbf{u} = 0, \qquad \mathbf{u} \cdot \nabla^* \mathbf{u} = \nabla^* p^{(0)},$$

since $\lambda^{*(0)} = \lambda^{*(0)}(\Psi^{*(0)})$ and thus $\mathbf{v}^{*(0)} \cdot \nabla^* \lambda^{*(0)} = 0$. Thus $\mathbf{u}$ may be considered the velocity field of an associated flow problem with stream function $\tilde{\Psi}$ and whose vorticity $\tilde{\mathbf{w}} = (0, 0, -\nabla^{*2} \tilde{\Psi})$ is constant along streamlines. Potential flow is an important class of solutions, the relevant solution that is zero along $\theta = 0$ and π/α being $\tilde{\Psi} = \tilde{c}_0 R^{*\alpha} \sin(\alpha\theta)$ with $\tilde{c}_0$ an arbitrary multiplicative constant. Assuming that the potentials are related by a power law behaviour of the form

$$c_0 \left(\frac{\tilde{\Psi}}{\tilde{c}_0}\right)^n = \Psi^{*(0)}$$

for some n and arbitrary constant c_0 we obtain

$$\Psi^{*(0)} = c_0 R^{*n\alpha}\sin^n(\alpha\theta), \qquad \lambda^{*(0)} = c_1\left(\frac{\Psi^{*(0)}}{c_0\alpha^n}\right)^{\frac{2(1-n)}{n}}, \tag{2.10}$$

where $c_1 = \tilde{c}_0^2/(nc_0\alpha^{n-1})^2$ is another arbitrary constant. Immediately from (2.8) we have that

$$d_1 = c_1, \qquad n_1 = \frac{2(1-n)}{n}.$$

For matching purposes we note the limiting behaviour of (2.10) as $\theta \to 0$ namely

$$\text{as } Y^* \to 0 \quad \Psi^{*(0)} \sim C_0 X^{*n(\alpha-1)} Y^{*n}, \;\; \lambda^{*(0)} \sim \frac{C_1}{n^2 C_0^2} X^{*2(n-1)(1-\alpha)} Y^{*2(1-n)}, \;\; p^{*(0)} \sim \frac{1}{2} C_1 X^{*-2(1-\alpha)}, \tag{2.11}$$

with C_0, C_1 and p_0 defined as

$$C_0 = c_0\alpha^n, \qquad C_1 = c_1 n^2 C_0^2. \tag{2.12}$$

The behaviour (to within an additive arbitrary constant) for $p^{*(0)}$ being obtained from the leading order balance in the momentum equation.

3. General boundary layer analysis

Taking inner variables

$$x = \epsilon\bar{X}, \qquad y = \epsilon^{2-\alpha}\bar{Y}, \qquad \psi = \epsilon^{3-\alpha}\bar{\Psi},$$

$$p = \epsilon^{-2(1-\alpha)}\bar{p}, \qquad T_{11} = \epsilon^{-2(1-\alpha)}\bar{T}_{11}, \qquad T_{12} = \epsilon^{-(1-\alpha)}\bar{T}_{12}, \qquad T_{22} = \bar{T}_{22},$$

we additionally introduce

$$u = \epsilon\bar{u}, \;\; v = \epsilon^{2-\alpha}\bar{v}, \;\; \lambda = \epsilon^{-2(2-\alpha)}\bar{\lambda}, \;\; \mu = \epsilon^{-(1-\alpha)}\bar{\mu}, \;\; \nu = \epsilon^2\bar{\nu}, \tag{3.1}$$

with

$$\bar{u} = \frac{\partial\bar{\Psi}}{\partial\bar{Y}}, \qquad \bar{v} = -\frac{\partial\bar{\Psi}}{\partial\bar{X}}.$$

Equivalently, relating outer and inner variables directly, we have

$$X^* = \bar{X}, \qquad Y^* = \epsilon^{1-\alpha}\bar{Y}, \qquad \Psi^* = \epsilon^{n(1-\alpha)}\bar{\Psi},$$

$$p^* = \bar{p}, \qquad T_{11}^* = \bar{T}_{11}, \qquad T_{12}^* = \epsilon^{(1-\alpha)}\bar{T}_{12}, \qquad T_{22}^* = \epsilon^{2(1-\alpha)}\bar{T}_{22},$$

$$u^* = \epsilon^{2-n\alpha}\bar{u}, \qquad v^* = \delta\epsilon^{1-\alpha}\bar{v}, \qquad \lambda^* = \epsilon^{-2(2-\alpha)(1-\alpha)}\bar{\lambda}, \qquad \mu^* = \epsilon^{-(1-\alpha)^2}\bar{\mu}, \qquad \nu^* = \epsilon^{2(1-\alpha)}\bar{\nu}. \tag{3.2}$$

The scaling for $\bar{\lambda}$ follows from (2.11), whilst those for $\bar{\mu}$ and $\bar{\nu}$ can be deduced from (1.15) and (1.8), when these expressions are written in inner variables and matching is to take place. Then (2.6) (or equivalently (1.7)) becomes

$$\bar{T}_{11} = -\epsilon^{2(1-\alpha)} + \bar{\lambda}\bar{u}^2 - \epsilon^{2(1-\alpha)}2\bar{\mu}\bar{u}\bar{v}\left(\bar{u}^2 + \epsilon^{2(1-\alpha)}\bar{v}^2\right)^{-1} + \epsilon^{4(1-\alpha)}\bar{\nu}\bar{v}^2\left(\bar{u}^2 + \epsilon^{2(1-\alpha)}\bar{v}^2\right)^{-2},$$

$$\bar{T}_{12} = \bar{\lambda}\bar{u}\bar{v} + \bar{\mu}\left(\bar{u}^2 - \epsilon^{2(1-\alpha)}\bar{v}^2\right)\left(\bar{u}^2 + \epsilon^{2(1-\alpha)}\bar{v}^2\right)^{-1} - \epsilon^{2(1-\alpha)}\bar{\nu}\bar{u}\bar{v}\left(\bar{u}^2 + \epsilon^{2(1-\alpha)}\bar{v}^2\right)^{-2},$$

$$\bar{T}_{22} = -1 + \bar{\lambda}\bar{v}^2 + 2\bar{\mu}\bar{u}\bar{v}\left(\bar{u}^2 + \epsilon^{2(1-\alpha)}\bar{v}^2\right)^{-1} + \bar{\nu}\bar{u}^2\left(\bar{u}^2 + \epsilon^{2(1-\alpha)}\bar{v}^2\right)^{-2}.$$

Thus, to leading order we have

$$\bar{T}_{11} = \bar{\lambda}\bar{u}^2, \quad \bar{T}_{12} = \bar{\lambda}\bar{u}\bar{v} + \bar{\mu}, \quad \bar{T}_{22} = -1 + \bar{\lambda}\bar{v}^2 + \frac{2\bar{\mu}\bar{v}}{\bar{u}} + \frac{\bar{\nu}}{\bar{u}^2}, \tag{3.3}$$

which relates the leading order Cartesian and natural stress variables within the boundary layer. These are precisely the relationships derived by Renardy [6]. The momentum equations now become

$$\begin{aligned}
\mathrm{Re}\,\epsilon^{2\alpha(2-\alpha)}\,\delta^2\,\bar{\mathbf{v}}\cdot\bar{\nabla}\bar{u} &= -\frac{\partial\bar{p}}{\partial\bar{X}} + \bar{\mathbf{v}}\cdot\bar{\nabla}(\bar{\lambda}\bar{u}) + \frac{\partial}{\partial\bar{Y}}\left(\bar{\mu}\frac{(\bar{u}^2 - \epsilon^{2(1-\alpha)}\bar{v}^2)}{(\bar{u}^2 + \epsilon^{2(1-\alpha)}\bar{v}^2)}\right) - \epsilon^{2(1-\alpha)}\frac{\partial}{\partial\bar{X}}\left(\frac{2\bar{\mu}\bar{u}\bar{v}}{(\bar{u}^2 + \epsilon^{2(1-\alpha)}\bar{v}^2)}\right)\\
&\quad -\epsilon^{2(1-\alpha)}\frac{\partial}{\partial\bar{Y}}\left(\frac{\bar{\nu}\bar{u}\bar{v}}{(\bar{u}^2 + \epsilon^{2(1-\alpha)}\bar{v}^2)}\right) + \epsilon^{4(1-\alpha)}\frac{\partial}{\partial\bar{X}}\left(\frac{\bar{\nu}\bar{v}^2}{(\bar{u}^2 + \epsilon^{2(1-\alpha)}\bar{v}^2)}\right),\\
\mathrm{Re}\,\epsilon^{2\alpha(2-\alpha)}\delta^2\,\epsilon^{2(1-\alpha)}\,\bar{\mathbf{v}}\cdot\bar{\nabla}\bar{v} &= -\frac{\partial\bar{p}}{\partial\bar{Y}} + \epsilon^{2(1-\alpha)}\bar{\mathbf{v}}\cdot\bar{\nabla}(\bar{\lambda}\bar{v}) + \epsilon^{2(1-\alpha)}\frac{\partial}{\partial\bar{Y}}\left(\frac{2\bar{\mu}\bar{u}\bar{v}}{(\bar{u}^2 + \epsilon^{2(1-\alpha)}\bar{v}^2)}\right)\\
&\quad +\epsilon^{2(1-\alpha)}\frac{\partial}{\partial\bar{X}}\left(\frac{\bar{\mu}(\bar{u}^2 - \epsilon^{2(1-\alpha)}\bar{v}^2)}{(\bar{u}^2 + \epsilon^{2(1-\alpha)}\bar{v}^2)}\right) + \epsilon^{2(1-\alpha)}\frac{\partial}{\partial\bar{Y}}\left(\frac{\bar{\nu}\bar{u}^2}{(\bar{u}^2 + \epsilon^{2(1-\alpha)}\bar{v}^2)}\right)\\
&\quad -\epsilon^{4(1-\alpha)}\frac{\partial}{\partial\bar{X}}\left(\frac{\bar{\nu}\bar{u}\bar{v}}{(\bar{u}^2 + \epsilon^{2(1-\alpha)}\bar{v}^2)}\right),
\end{aligned}$$

whilst the constitutive equations take the form

$$\begin{aligned}
&\bar{\mathbf{v}}\cdot\bar{\nabla}\bar{\lambda} + \bar{\lambda} + 2\bar{\mu}\left(\frac{\partial}{\partial\bar{Y}}\left(\frac{\bar{u}}{\bar{u}^2 + \epsilon^{2(1-\alpha)}\bar{v}^2}\right) - \epsilon^{2(1-\alpha)}\frac{\partial}{\partial\bar{X}}\left(\frac{\bar{v}}{\bar{u}^2 + \epsilon^{2(1-\alpha)}\bar{v}^2}\right)\right) = \frac{\epsilon^{2(1-\alpha)}}{(\bar{u}^2 + \bar{v}^2)},\\
&\bar{\mathbf{v}}\cdot\bar{\nabla}\bar{\mu} + \bar{\mu} + \bar{\nu}\left(\frac{\partial}{\partial\bar{Y}}\left(\frac{\bar{u}}{\bar{u}^2 + \epsilon^{2(1-\alpha)}\bar{v}^2}\right) - \epsilon^{2(1-\alpha)}\frac{\partial}{\partial\bar{X}}\left(\frac{\bar{v}}{\bar{u}^2 + \epsilon^{2(1-\alpha)}\bar{v}^2}\right)\right) = 0,\\
&\bar{\mathbf{v}}\cdot\bar{\nabla}\bar{\nu} + \bar{\nu} = (\bar{u}^2 + \epsilon^{2(1-\alpha)}\bar{v}^2).
\end{aligned}$$

Consequently, in $\bar{X} = O(1), \bar{Y} = O(1)$, we have the leading order equations

$$0 = -\frac{d\bar{p}}{d\bar{X}} + \bar{\mathbf{v}}\cdot\bar{\nabla}(\bar{\lambda}\bar{u}) + \frac{\partial\mu}{\partial\bar{Y}},$$

with

$$\bar{\mathbf{v}}\cdot\bar{\nabla}\bar{\lambda} + \bar{\lambda} + 2\bar{\mu}\frac{\partial}{\partial\bar{Y}}\left(\frac{1}{\bar{u}}\right) = 0, \quad \bar{\mathbf{v}}\cdot\bar{\nabla}\bar{\mu} + \bar{\mu} + \bar{\nu}\frac{\partial}{\partial\bar{Y}}\left(\frac{1}{\bar{u}}\right) = 0, \quad \bar{\mathbf{v}}\cdot\bar{\nabla}\bar{\nu} + \bar{\nu} = \bar{u}^2, \tag{3.4}$$

which can be equivalently stated in terms of the stream function as

$$0=-\frac{d\bar{p}}{d\bar{X}}+\left(\frac{\partial\bar{\Psi}}{\partial\bar{Y}}\right)\frac{\partial}{\partial\bar{X}}\left(\bar{\lambda}\frac{\partial\bar{\Psi}}{\partial\bar{Y}}\right)-\left(\frac{\partial\bar{\Psi}}{\partial\bar{X}}\right)\frac{\partial}{\partial\bar{Y}}\left(\bar{\lambda}\frac{\partial\bar{\Psi}}{\partial\bar{Y}}\right)+\frac{\partial\bar{\mu}}{\partial\bar{Y}}, \tag{3.5}$$

$$\left(\frac{\partial\bar{\Psi}}{\partial\bar{Y}}\right)^2\left(\frac{\partial\bar{\Psi}}{\partial\bar{Y}}\frac{\partial\bar{\lambda}}{\partial\bar{X}}-\frac{\partial\bar{\Psi}}{\partial\bar{X}}\frac{\partial\bar{\lambda}}{\partial\bar{Y}}+\bar{\lambda}\right)-2\frac{\partial^2\bar{\Psi}}{\partial\bar{Y}^2}\bar{\mu}=0, \tag{3.6}$$

$$\left(\frac{\partial\bar{\Psi}}{\bar{X}}\right)^2\left(\frac{\partial\bar{\Psi}}{\partial\bar{Y}}\frac{\partial\bar{\mu}}{\partial\bar{X}}-\frac{\partial\bar{\Psi}}{\partial\bar{X}}\frac{\partial\bar{\mu}}{\partial\bar{Y}}+\bar{\mu}\right)-\frac{\partial^2\bar{\Psi}}{\partial\bar{Y}^2}\bar{\nu}=0, \tag{3.7}$$

$$\frac{\partial\bar{\Psi}}{\partial\bar{Y}}\frac{\partial\bar{\nu}}{\partial\bar{X}}-\frac{\partial\bar{\Psi}}{\partial\bar{X}}\frac{\partial\bar{\nu}}{\partial\bar{Y}}+\bar{\nu}-\left(\frac{\partial\bar{\Psi}}{\partial\bar{Y}}\right)^2=0. \tag{3.8}$$

The equations (3.4) were first recorded in [6] as a similarity solution of the high Weissenberg boundary layers, which clearly manifest themselves in the We $=1$ case in the presence of a re-entrant corner singularity. The leading order matching conditions for the natural stress variables are

$$\lim_{Y^*\to 0}\lambda^{*(0)}=\epsilon^{-2(2-\alpha)(1-\alpha)}\lim_{\bar{Y}\to\infty}\bar{\lambda}^{(0)},\quad \lim_{Y^*\to 0}\mu^{*(0)}=\epsilon^{-(1-\alpha)^2}\lim_{\bar{Y}\to\infty}\bar{\mu}^{(0)},\quad \lim_{Y^*\to 0}\nu^{*(0)}=\epsilon^{2(1-\alpha)}\lim_{\bar{Y}\to\infty}\bar{\nu}^{(0)},$$

which upon using (2.8) and writing the outer variables in terms of the inner gives immediately

$$\bar{\lambda}^{(0)}\sim d_1\left(\frac{\bar{\Psi}^{(0)}}{C_0}\right)^{n_1},\quad \bar{\mu}^{(0)}\sim d_2\left(\frac{\bar{\Psi}^{(0)}}{C_0}\right)^{n_2},\quad \bar{\nu}^{(0)}\sim d_3\left(\frac{\bar{\Psi}^{(0)}}{C_0}\right)^{n_3}\qquad \text{as } \bar{Y}\to\infty.$$

as well as

$$n_1=\frac{-2(2-\alpha)}{(3-\alpha)}=\frac{2(1-n)}{n},\quad n_2=\frac{-(1-\alpha)}{(3-\alpha)}=\frac{(2-n)}{n},\quad n_3=\frac{2}{(3-\alpha)}=\frac{2}{n},$$

on balancing powers of ϵ. The matching condition of the inner variables with those of the outer gives the behaviour

$$\text{as } \bar{Y}\to\infty\qquad \bar{\Psi}\sim C_0\bar{X}^{n(\alpha-1)}\bar{Y}^n,\quad \bar{\lambda}\sim d_1\bar{X}^{2(1-n)(\alpha-1)}\bar{Y}^{2(1-n)},\quad \bar{\mu}\sim d_2\bar{X}^{(2-n)(\alpha-1)}\bar{Y}^{2-n},$$
$$\bar{\nu}\sim d_3\bar{X}^{2(\alpha-1)}\bar{Y}^2,\quad \bar{p}\sim\frac{1}{2}C_1\bar{X}^{-2(1-\alpha)}. \tag{3.9}$$

The boundary layer equations are completed with the usual no slip and solid boundary conditions at the wall,

$$\text{on}\quad \bar{Y}=0,\quad \bar{\Psi}=\frac{\partial\bar{\Psi}}{\partial\bar{Y}}=0. \tag{3.10}$$

The equations (3.5)–(3.8) with far-field behaviour (3.9) and wall conditions (3.10) possess the similarity solution

$$\xi=\frac{\bar{Y}}{\bar{X}^{2-\alpha}},\quad \bar{\Psi}=\bar{X}^{3-\alpha}f(\xi),\quad \bar{p}=p_0\bar{X}^{-2(1-\alpha)},$$

$$\bar{\lambda}=\bar{X}^{-2(2-\alpha)}\tilde{\lambda}(\xi),\quad \bar{\mu}=\bar{X}^{\alpha-1}\tilde{\mu}(\xi),\quad \bar{\nu}=\bar{X}^2\tilde{\nu}(\xi), \tag{3.11}$$

which give the reduced system

$$0 = \tilde{\mu}' + 2(1-\alpha)p_0 + \frac{2f''}{f'}\tilde{\mu} - \left(f'(1-f') + (3-\alpha)ff''\right)\tilde{\lambda}, \tag{3.12}$$

$$(3-\alpha)f\tilde{\lambda}' + (2(2-\alpha)f' - 1)\tilde{\lambda} + 2\frac{f''}{f'^2}\tilde{\mu} = 0, \tag{3.13}$$

$$(3-\alpha)f\tilde{\mu}' + ((1-\alpha)f' - 1)\tilde{\mu} + \frac{f''}{f'^2}\tilde{\nu} = 0, \tag{3.14}$$

$$(3-\alpha)f\tilde{\nu}' - (1+2f')\tilde{\nu} + f'^2 = 0, \tag{3.15}$$

$$\text{at } \xi = 0 \qquad f = f' = 0, \tag{3.16}$$

$$\text{as } \xi \to \infty \qquad f \sim C_0\xi^{3-\alpha}, \quad \tilde{\lambda}(\xi) \sim d_1\xi^{-2(2-\alpha)}, \quad \tilde{\mu}(\xi) \sim d_2\xi^{-1+\alpha}, \quad \tilde{\nu}(\xi) \sim d_3\xi^2. \tag{3.17}$$

The constant p_0 satisfies

$$p_0 = \frac{1}{2}C_1 \tag{3.18}$$

which is immediate from (3.9) and (3.11). The equations (3.12)–(3.15) are related to the Cartesian formulation (see section 3.2 in [1]) by the transformation

$$\begin{aligned}
\tilde{\lambda}(\xi) &= \frac{t_{11}(\xi)}{f'(\xi)^2}, \\
\tilde{\mu}(\xi) &= t_{12}(\xi) + \frac{t_{11}(\xi)}{f'(\xi)}((3-\alpha)f(\xi) - (2-\alpha)\xi f'(\xi)), \\
\tilde{\nu}(\xi) &= (1 + t_{22}(\xi))f'(\xi)^2 + t_{11}(\xi)((3-\alpha)f(\xi) - (2-\alpha)\xi f'(\xi))^2 \\
&\qquad + 2t_{12}(\xi)f'(\xi)((3-\alpha)f(\xi) - (2-\alpha)\xi f'(\xi)),
\end{aligned} \tag{3.19}$$

which follows from (3.3) on using similarity variables, where

$$\bar{T}_{11} = \bar{X}^{2(\alpha-1)}t_{11}(\xi), \qquad \bar{T}_{12} = \bar{X}^{(\alpha-1)}t_{12}(\xi), \qquad \bar{T}_{22} = t_{22}(\xi),$$

One notable feature of the boundary layer equations (3.12)–(3.15) in similarity variables of the natural stress basis, is that they are autonomous and can be reduced (through choice of f as the new dependent variable) to a fourth order system. However, we do not exploit this reduction here.

Analogous to the Cartesian case, the equations (3.12)–(3.15) have the local wall behaviour

$$\text{as } \xi \to 0 \qquad \begin{aligned}
f(\xi) &= \frac{1}{2}a\xi^2 + \frac{1}{3!}b\xi^3 + \frac{1}{4!}3(1-\alpha)^2a^3\xi^4 + O(\xi^5), \\
\tilde{\lambda}(\xi) &= 2\xi^{-2} + \frac{2}{a}(b + 3(1-\alpha)a^2)\xi^{-1} + O(1), \\
\tilde{\mu}(\xi) &= a + (b + 2(1-\alpha)a^2)\xi + O(\xi^2), \\
\tilde{\nu}(\xi) &= a^2\xi^2 + a(b + (1-\alpha)a^2)\xi^3 + O(\xi^4),
\end{aligned} \tag{3.20}$$

where $a = f''(0), b = f'''(0)$ and p_0 additionally satisfies

$$p_0 = \frac{1}{2}a^2 + \frac{1}{2(\alpha-1)}b. \tag{3.21}$$

Following the discussion in section 3.1 of [1], this expansion is analytic for $a < 0$ but non-analytic for $a > 0$ where subdominant exponentially small terms are present (which are derived in Appendix A).

Comparing (3.17) with the far-field expressions derived in section 3.2 of [1], gives the far-field parameters d_1, d_2, d_3 in terms of the Cartesian expansion parameters C_0, C_1, C_4, C_5. In the particular case $C_4 = 0$ (which appears to hold uniformly from the numerical results in [1] for our two parameter family of solutions, irrespective of the corner angle) these are

$$d_1 = \frac{C_1}{(3-\alpha)^2 C_0^2}, \quad d_2 = \frac{C_1}{2(3-\alpha)C_0}, \quad d_3 = \left(\frac{C_1}{4} + \frac{2C_1C_0^2C_5(3-\alpha)(3-2\alpha)}{\alpha}\right). \tag{3.22}$$

It is worth recording that (3.17) and (3.22) give

$$\tilde{\lambda}\tilde{\nu} - \tilde{\mu}^2 \sim \Delta_0 \xi^{-2+2\alpha} \qquad \text{as } \xi \to \infty,$$

where

$$\Delta_0 = d_1 d_3 - d_2^2 = \frac{2(3-2\alpha)}{\alpha(3-\alpha)} C_1^2 C_5.$$

We also note that we may use (3.14) in (3.12) to give an expression for f'' as

$$f'' = f'^2 \frac{\left((3-\alpha)ff'(f'-1)\tilde{\lambda} + (1-(1-\alpha)f')\tilde{\mu} + 2(1-\alpha)(3-\alpha)p_0 f\right)}{\left((3-\alpha)^2 f^2 f'^2 \tilde{\lambda} - 2(3-\alpha)ff'\tilde{\mu} + \tilde{\nu}\right)}, \tag{3.23}$$

which will useful when forming an explicit system of equations for numerical implementation.

4. The parametric solution dependence

4.1 The upstream boundary layer

To consider solutions for the upstream layer, we introduce the label u to the wall and far-field constants as follows

$$(a, b, p_0, C_0, C_1, C_5, d_1, d_2, d_3) = (a_u, b_u, p_{0u}, C_{0u}, C_{1u}, C_{5u}, d_{1u}, d_{2u}, d_{3u}), \tag{4.1}$$

in keeping with the notation introduced in [1]. The far-field parameters in (4.1) are related to those of the Cartesian stress far-field expansions through the expressions (3.22) with the appropriate u label introduced, namely,

$$d_{1u} = \frac{C_{1u}}{(3-\alpha)^2 C_{0u}^2}, \quad d_{2u} = \frac{C_{1u}}{2(3-\alpha)C_{0u}}, \quad d_{3u} = \left(\frac{C_{1u}}{4} + \frac{2C_{1u}C_{0u}^2C_{5u}(3-\alpha)(3-2\alpha)}{\alpha}\right). \tag{4.2}$$

In addition we have from (3.18) that

$$C_{1u} = 2p_{0u}.$$

The initial value problem for the upstream layer in the natural stress variables is now to solve (3.12)–(3.15) over the interval $[\xi_0, \xi_\infty]$ with a pre-determined number of terms in the expansion

(3.20) imposed at a small positive but non-zero value $\xi = \xi_0$. Using the variables f, f', λ, μ, ν we may formulate an explicit fifth order system of first order ODEs composed of (3.13)–(3.15) with (3.23). As initial conditions we take

$$\text{at } \xi = \xi_0 \qquad f = \frac{1}{2}a_u\xi_0^2 + \frac{1}{6}b_u\xi_0^3, \quad f' = a_u\xi_0 + \frac{1}{2}b_u\xi_0^2,$$
$$\tilde{\lambda} = 2\xi_0^{-2} + \frac{2}{a_u}\left(b_u + 3(1-\alpha)a_u^2\right)\xi_0^{-1}, \quad \tilde{\mu} = a_u + \left(b_u + 2(1-\alpha)a_u^2\right)\xi_0,$$
$$\tilde{\nu} = a_u^2\xi_0^2 + a_u\left(b_u + (1-\alpha)a_u^2\right)\xi_0^3, \tag{4.3}$$

where (3.21) gives

$$b_u = (1-\alpha)\left(a_u^2 - 2p_{0u}\right).$$

For numerical implementation it is more convenient to use scaled variables

$$\ell(\xi) = \xi^2\tilde{\lambda}(\xi), \quad m(\xi) = \tilde{\mu}(\xi), \quad n(\xi) = \frac{\tilde{\nu}(\xi)}{\xi^2}, \tag{4.4}$$

which is advantageous for both the wall and far-field behaviours (3.20) and (3.17). This scaling is similar to the one used by [3], who chose to use f'^2 to scale $\tilde{\lambda}$ and $\tilde{\nu}$. The IVP is solved using MATLAB's ode15s with error tolerances RelTol= 10^{-13} and AbsTol= 10^{-13}. A comprehensive discussion of the solution to the upstream case in the Cartesian variables was given in [1]. Here we add to these results, noting how the numerical solution in the natural stress variables compares and recording the relevant parameter results.

A) Comparison with the Cartesian stress formulation results. We use the parameter case $a_u = -1, p_{0u} = 1, \alpha = 2/3$ with $\xi_0 = 10^{-6}, \xi_\infty = 10^6$. Figure 1 shows the solution profiles. Estimates of the far-field constants $C_{0u}, d_{1u}, d_{2u}, d_{3u}$ are recorded in Table 1 using the far-field behaviours (3.17) evaluated at selected ξ_∞. The analytical expressions (4.2) for d_{1u} and d_{2u} are also evaluated using the C_{0u} estimate, confirming these expressions in this case. Comparison with the values for $C_{0u}, d_{1u}, d_{2u}, d_{3u}$ using the Cartesian formulation given in Tables 1 and 3 of Appendix B in [1], shows very good agreement (at least 4 d.p.).

B) Parameter dependencies for $a_u = -1$. As described in [1], it is sufficient to consider the parameter case $a_u = -1$ only, all other values of negative a_u (including $a_u = 0$) then being deducible. Figure 2 shows estimates of the far-field constants $C_{0u}, d_{1u}, d_{2u}, d_{3u}$ over a range of p_{0u} in the case $a_u = -1$ for selected corner angles α.

In the limit $p_{0u} \to +\infty$ we have from [1] that

$$C_{0u} \sim k_0 p_{0u}^{1-\frac{\alpha}{2}}, \qquad C_{5u} \sim \frac{k_5}{p_{0u}^{2-\alpha}}. \tag{4.5}$$

It then follows from (4.2) that

$$d_{1u} \sim \kappa_1 p_{0u}^{\alpha-1}, \quad d_{2u} \sim \kappa_2 p_{0u}^{\frac{\alpha}{2}}, \quad d_{3u} \sim \kappa_3 p_{0u}, \tag{4.6}$$

where

$$\kappa_1 = \frac{2}{(3-\alpha)^2k_0^2}, \quad \kappa_2 = \frac{1}{(3-\alpha)k_0}, \quad \kappa_3 = \left(\frac{1}{2} + \frac{4k_0^2k_5(3-\alpha)(3-2\alpha)}{\alpha}\right). \tag{4.7}$$

Estimates of $k_0, \kappa_1, \kappa_2, \kappa_3$ are shown in Figure 3.

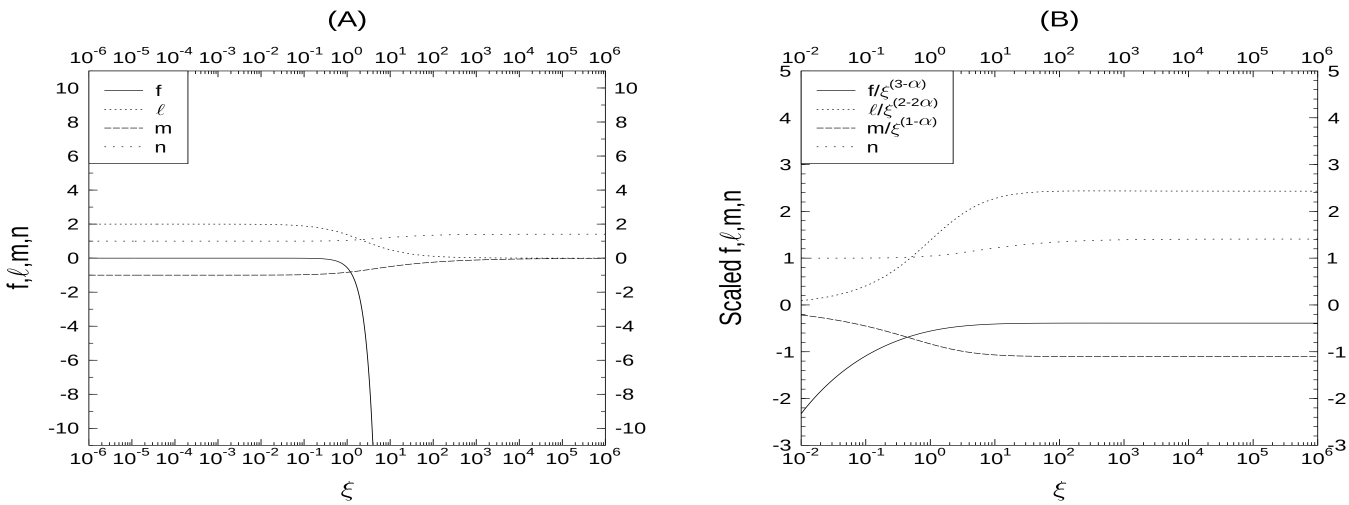

Figure 1: Solution profiles in the natural stress formulation of the IVP for the upstream boundary layer. Scheme parameters used were $a_u = -1, p_{0u} = 1, \alpha = 2/3, \xi_0 = 10^{-6}, \xi_\infty = 10^6$. The related natural stress variables ℓ, m, n as defined in (4.4) are shown in (A) and scaled with their far-field behaviours in (B) to illustrate convergence.

$a_u = -1, p_{0u} = 1, \alpha = 2/3$						
	C_{0u} estimates	d_{1u} estimates		d_{2u} estimates		d_{3u} estimates
ξ_∞	$f\xi^{\alpha-3}$	$\tilde{\lambda}\xi^{4-2\alpha}$	$\frac{C_{1u}}{(3-\alpha)^2 C_{0u}^2}$	$\tilde{\mu}\xi^{1-\alpha}$	$\frac{C_{1u}}{2(3-\alpha)C_{0u}}$	$\tilde{\nu}\xi^{-2}$
10^2	-0.38850911	2.43132663	2.43373911	-1.10105777	-1.10311811	1.34694694
10^3	-0.38806823	2.43586525	2.43927204	-1.10278031	-1.10437132	1.39273533
10^4	-0.38848973	2.43290919	2.43398188	-1.10268464	-1.10317312	1.40459292
10^5	-0.38863918	2.43184298	2.43211030	-1.10262759	-1.10274891	1.40735040
10^6	-0.38867756	2.43156868	2.43163001	-1.10261220	-1.10264002	1.40796469
10^7	-0.38868646	2.43150505	2.43151864	-1.10260860	-1.10261477	1.40809905
10^8	-0.38868844	2.43149089	2.43149385	-1.10260780	-1.10260915	1.40812820

Table 1: Estimates of far-field constants in the case $a_u = -1, p_{0u} = 1, \alpha = 2/3$. Shown are estimates of the far-field constants $C_{0u}, d_{1u}, d_{2u}, d_{3u}$ in the natural stress basis formulation of the IVP. The far-field behaviour (3.17) is used to provide estimates by evaluating the stated functions at selected ξ_∞ values. Comparison with theoretical estimates of d_{1u}, d_{2u} from (4.2) are also recorded. Convergence with increasing ξ_∞ is evident.

4.2 The downstream boundary layer

To consider solutions of the downstream layer, we introduce the label d to the wall and far-field parameters as follows

$$(a, b, p_0, C_0, C_1, C_5, d_1, d_2, d_3) = (a_d, b_d, p_{0d}, C_{0d}, C_{1d}, C_{5d}, d_{1d}, d_{2d}, d_{3d}), \tag{4.8}$$

where

$$C_{1d} = 2p_{0d}, \qquad b_u = (1-\alpha)\left(a_u^2 - 2p_{0u}\right).$$

The downstream layer far-field parameters of the natural and Cartesian stress bases are related by

$$d_{1d} = \frac{C_{1d}}{(3-\alpha)^2 C_{0d}^2},\ d_{2d} = \frac{C_{1d}}{2(3-\alpha)C_{0d}},\ d_{3d} = \left(\frac{C_{1d}}{4} + \frac{2C_{1d}C_{0d}^2 C_{5d}(3-\alpha)(3-2\alpha)}{\alpha}\right). \tag{4.9}$$

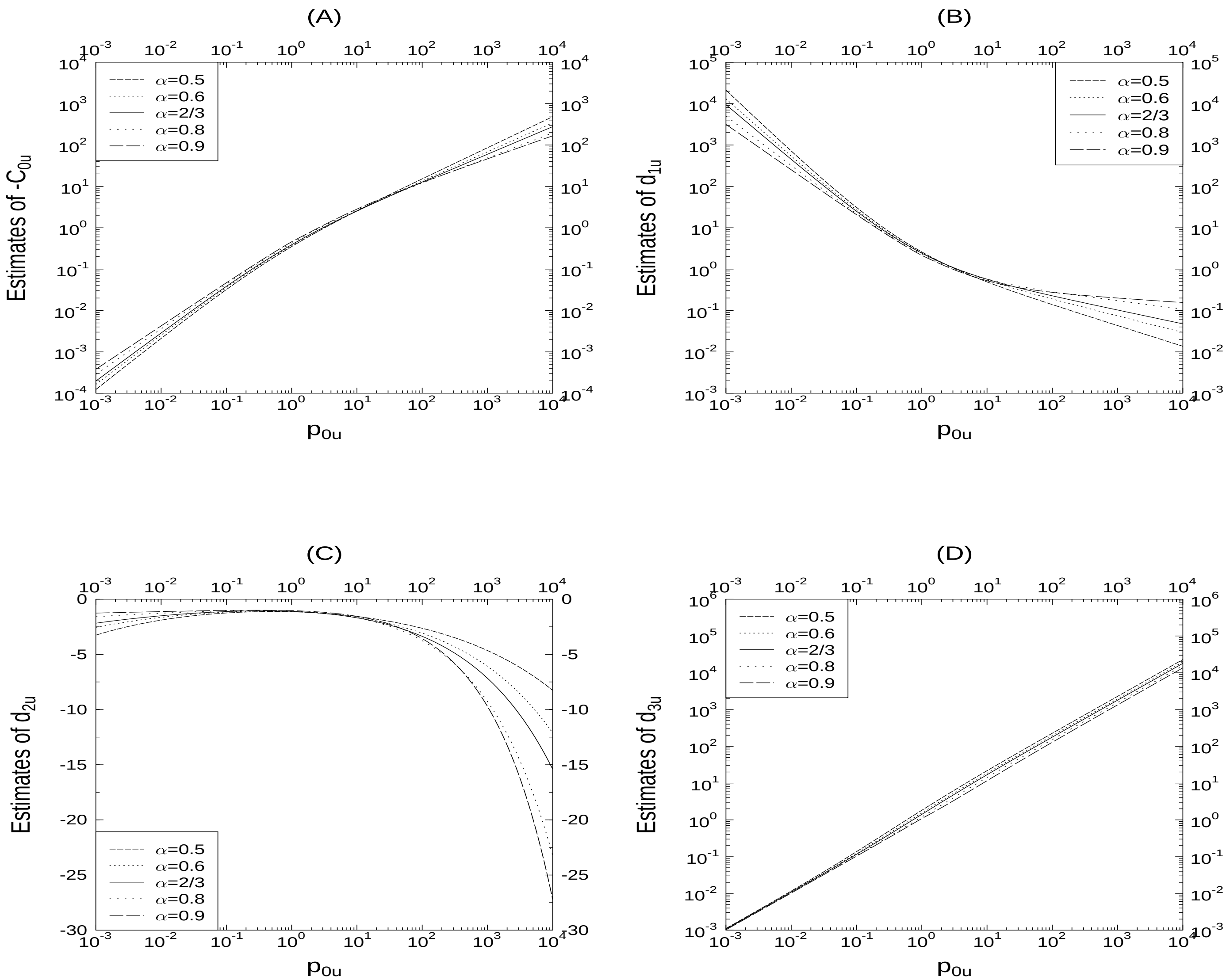

Figure 2: Estimates of the far-field constants $C_{0u}, d_{1u}, d_{2u}, d_{3u}$ over a range of p_{0u} in the case $a_u = -1$ for selected corner angles α. The IVP was solved with scheme parameters $\xi_0 = 10^{-6}, \xi_\infty = 10^6$. For $p_{0u} = o(1)$, significantly larger values of ξ_∞ are required, with the value 10^{30} being used for $p_{0u} = 10^{-3}$.

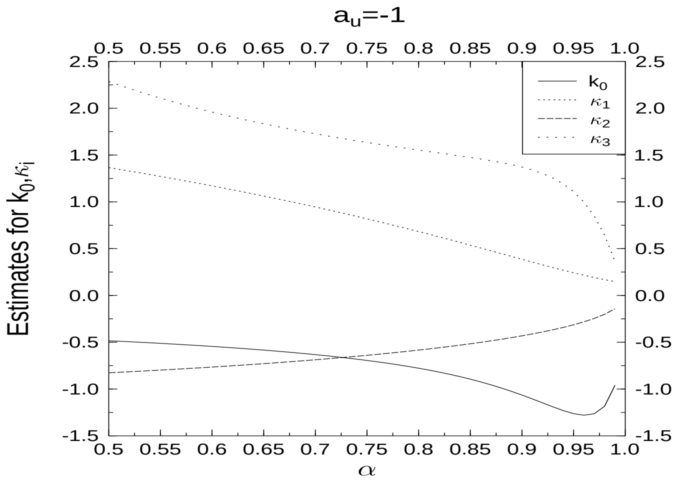

Figure 3: Estimates of the coefficients $k_0, \kappa_1, \kappa_2, \kappa_3$ with the corner angle parameter α in the asymptotic relationships (4.5) and (4.6). The IVP was solved with $a_u = -1, p_{0u} = 10^5, \xi_0 = 10^{-6}, \xi_\infty = 10^6$. The estimates of κ_1 and κ_2 using $\tilde{\lambda}$ and $\tilde{\mu}$ from the numerical scheme and those from (4.7) (with k_0 from C_{0u}) agreed to 6 d.p.

Additionally, the upstream and downstream far-field parameters are related by

$$p_{0d} = p_{0u}, \qquad C_{0d} = -C_{0u}, \qquad d_{1d} = d_{1u}, \qquad d_{2d} = -d_{2u}, \qquad d_{3d} = d_{3u}, \tag{4.10}$$

which follow from (1.12) and (2.8), so that

$$d_{1d} = \frac{2p_{0u}}{(3-\alpha)^2 C_{0u}^2}, \; d_{2d} = -\frac{p_{0u}}{(3-\alpha)C_{0u}}, \; d_{3d} = \left(\frac{p_{0u}}{2} + \frac{4p_{0u}C_{0u}^2 C_{5u}(3-\alpha)(3-2\alpha)}{\alpha}\right). \tag{4.11}$$

The boundary value problem for the downstream layer in the natural stress variables is to solve the explicit fifth order system (3.13)–(3.15) and (3.23) with the asymptotic behaviour (3.17) imposed at $\xi = \xi_\infty$ and (3.20) imposed at $\xi = \xi_0$. The formulation BVP2 in section 4.2 of [1] requires that the parameters $(p_{0d}, C_{0d}, d_{2d}, d_{3d})$ are prescribed whilst the wall parameter a_d is to be determined. We note that prescribing d_{1d} is not necessary and specifying $\tilde{\lambda}$ in the far-field does not impose a condition on our system (see the first eigenmode in Appendix B). MATLAB's bvp4c solver is used to solve the system numerically over the interval $[\xi_0, \xi_\infty]$, where as boundary conditions we take

$$\begin{aligned} &\text{at } \xi = \xi_0 \qquad && f = \frac{1}{2}\tilde{\mu}\xi_0^2, \quad \tilde{\nu} = \tilde{\mu}^2\xi_0^2, \\ &\text{at } \xi = \xi_\infty \qquad && f = C_{0d}\xi_\infty^{3-\alpha}, \quad \tilde{\mu} = d_{2d}\xi_\infty^{\alpha-1}, \quad \tilde{\nu} = d_{3d}\xi_\infty^2. \end{aligned} \tag{4.12}$$

Again it is convenient to use the variables ℓ, m, n as defined in (4.4) in place of $\tilde{\lambda}, \tilde{\mu}, \tilde{\nu}$ so that the boundary conditions become

$$\begin{aligned} &\text{at } \xi = \xi_0 \qquad && f = \frac{1}{2}m\xi_0^2, \quad n = m^2, \\ &\text{at } \xi = \xi_\infty \qquad && f = C_{0d}\xi_\infty^{3-\alpha}, \quad m = d_{2d}\xi_\infty^{\alpha-1}, \quad n = d_{3d}. \end{aligned} \tag{4.13}$$

The solver bvp4c is implemented with default error tolerances RelTol= 10^{-3},AbsTol= 10^{-6}, vectorization and the initial solution guess

$$f = \begin{cases} \frac{1}{2}a_d\xi^2 + (C_{0d} - \frac{1}{2}a_d)\xi^3, & \xi \le 1, \\ C_{0d}\xi^{(3-\alpha)}, & \xi > 1, \end{cases} \qquad f' = \begin{cases} a_d\xi + (C_{0d}(3-\alpha) - a_d)\xi^2, & \xi \le 1, \\ C_{0d}(3-\alpha)\xi^{(2-\alpha)}, & \xi > 1, \end{cases}$$

$$\ell = \begin{cases} 2 + (d_{1d} - 2)\xi, & \xi \le 1, \\ d_{1d}, & \xi > 1, \end{cases} \quad m = \begin{cases} a_d + (d_{2d} - a_d)\xi, & \xi \le 1, \\ d_{2d}\xi^{\alpha-1}, & \xi > 1, \end{cases}$$

$$n = \begin{cases} a_d^2 + (d_{3d} - a_d^2)\xi, & \xi \le 1, \\ d_{3d}, & \xi > 1. \end{cases}$$

The initial guess solution is posed on an interval with $\xi_0 = 10^{-1}, \xi_\infty = 10$ and 500 equally spaced mesh points. Continuation is then used with MATLAB's bvpinit to extend the solution to a larger interval with $\xi_0 = 10^{-3}, \xi_\infty = 10^4$. The parameter values $(p_{0d}, C_{0d}, d_{2d}, d_{3d})$ are set by relating them to the upstream values using (4.10), where for given (a_u, p_{0u}, α) the IVP of section 4.1 is solved to obtain estimates of (C_{0u}, d_{2u}, d_{3u}) (here used with $\xi_0 = 10^{-6}$ and $\xi_\infty = 10^6$). In addition, the initial guess solution requires an estimate of a_d which is taken as 1 for the case $a_u = -1, p_{0u} = 1, \alpha = 2/3$.

Figure 4(A) and (B) shows the solution profile and convergence of estimates of a_d respectively in the parameter case $a_u = -1, p_{0u} = 1, \alpha = 2/3$. Figure 4(B) plots five possible functions from which estimates of a_d can be determined. These estimates are consistent to two decimal places as recorded in the figure legend.

Figure 5(A) and (B) show the behaviour of estimates of a_d from the numerical scheme as p_{0d} varies for the parameter case $a_u = -1, p_{0u} = p_{0d}, \alpha = 2/3$. Also plotted is the large p_{0d} asymptotic behaviour

$$a_d = k_d\, p_{0d}^{1/2}, \tag{4.14}$$

noted in section 4.2 of [1]. The constant k_d is obtained numerically from the value of the ratio $a_d/p_{0d}^{1/2}$ at large p_{0d}. At $p_{0d} = 10^5$, we have the value $k_d \approx 2.6219$ using $f''(\xi_0)$. Figure 5(A) shows the numerical and analytical approximation (4.14) over relatively small values of p_{0d}, whilst Figure 5(B) gives a larger range of p_{0d} values and makes use of log scales. The asymptotic approximation (4.14) is approached relatively rapidly and appears to hold well for p_{0d} in excess of 10^2. Figure 5(A) strongly suggests a constant as a correction term to (4.14). Another important observation is that in the $\alpha = 2/3$ case then $p_{0d} \approx 0.5$ is the value at which the magnitude of the downstream parameter a_d equals that of the upstream. If p_{0d} exceeds (is less than) this value then the magnitude of the downstream shear rate exceeds (or is less than) that of the upstream shear rate.

Finally, Figure 5(C) and (D) gives estimates of a_d and k_d for other re-entrant corner angles. Estimates were difficult to obtain for α in excess of 0.975.

5. Solution summary

For a given re-entrant corner angle, i.e. fixed $\alpha \in [1/2, 1)$, the local asymptotic solution can be expressed in terms of the two upstream parameters a_u and p_{0u}. The upstream boundary layer equations can be solved as an IVP as described in section 4.1 to determine the upstream far-field constants $C_{0u}, d_{1u}, d_{2u}, d_{3u}$. These are then communicated unchanged through the outer core flow and fed into the downstream boundary layer. Allowing for a change in axes orientation, the downstream boundary layer equations are the same as the upstream boundary layer equations, the only difference being with a change of sign for certain of the far-field coefficients (see (4.10)). For given values of $p_{0d}, C_{0d}, d_{2d}, d_{3d}$ (the value of d_{1d} being always automatically determined by p_{0d} and C_{0d}) then the two-point BVP for the downstream layer can be solved as described in section 4.2. In particular, the downstream parameter a_d can be determined.

The description of this two parameter solution is facilitated through a scaling invariance for the problem which allows for the solution for any $a_u < 0$ to be mapped onto the $a_u = -1$ case. Specifically, for a given α, we denote the parameter values with hats as follows

$$p_{0u} = \hat{p}_{0u}, \quad C_{0u} = \hat{C}_{0u}, \quad d_{1u} = \hat{d}_{1u}, \quad d_{2u} = \hat{d}_{2u}, \quad d_{3u} = \hat{d}_{3u},$$

$$p_{0d} = p_{0u}, \quad C_{0d} = -C_{0u}, \quad d_{1d} = \hat{d}_{1u}, \quad d_{2d} = -\hat{d}_{2u}, \quad d_{3d} = \hat{d}_{3u}, \quad a_d = \hat{a}_d, \tag{5.1}$$

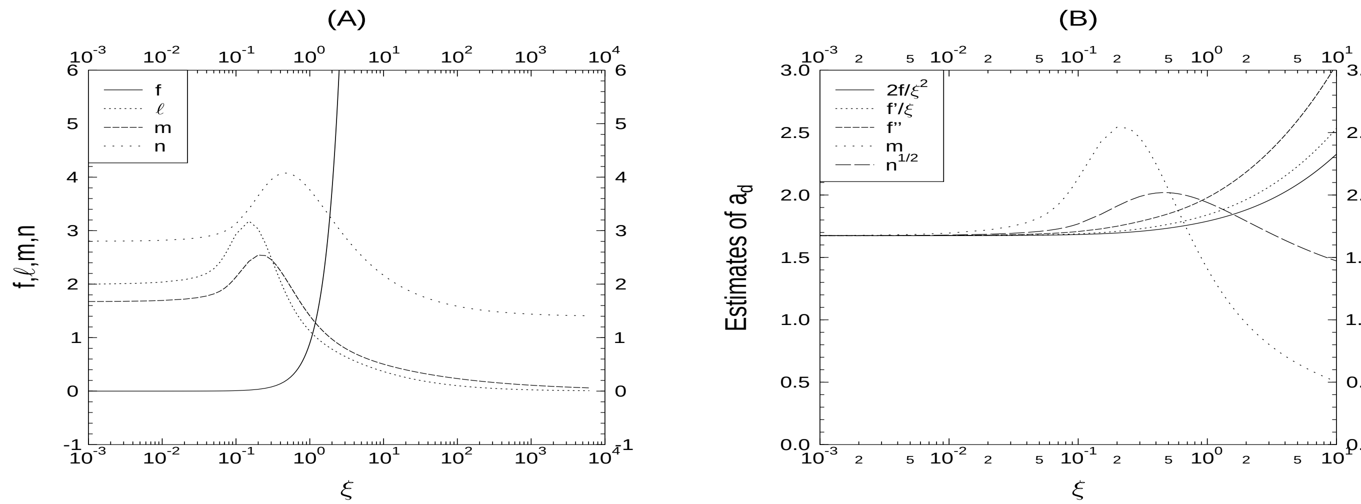

Figure 4: Illustration of the solution and estimates for a_d in the case $a_u = -1, p_{0u} = 1, \alpha = 2/3$. Maximum residual 3.6×10^{-4}. (A) shows the solution profiles. (B) shows the behaviour for small ξ of the variables $2f/\xi^2, f'/\xi, f'', m, n^{1/2}$ all of which give estimates of a_d. Numerically we have at $\xi_0 = 10^{-3}$ that $2f/\xi^2 = 1.674561..., f'/\xi = 1.674561..., f'' = 1.673157..., m = 1.675027..., n^{1/2} = 1.675027....$

when $a_u = -1$. Then, the parameter values for other $a_u \neq 0$ values are given by

$$p_{0u} = (-a_u)^2\hat{p}_{0u}, \quad C_{0u} = (-a_u)^{2-\alpha}\hat{C}_{0u}, \quad d_{1u} = (-a_u)^{2(\alpha-1)}\hat{d}_{1u}, \quad d_{2u} = (-a_u)^{\alpha}\hat{d}_{2u}, \quad d_{3u} = (-a_u)^2\hat{d}_{3u},$$

$$p_{0d} = p_{0u}, \quad C_{0d} = -C_{0u}, \quad d_{1d} = d_{1u}, \quad d_{2d} = -d_{2u}, \quad d_{3d} = d_{3u}, \quad a_d = (-a_u)^2\hat{a}_d. \tag{5.2}$$

We note that explicit expressions exist for d_{1u} and d_{2u} in terms of p_{0u}, C_{0u} as given by (4.2). Figure 4 shows parameter plots of $C_{0u}, d_{1u}, d_{2u}, d_{3u}$ with p_{0u} in the case $a_u = -1$ for selected α. A plot of a_d in the case $a_u = -1$ for $\alpha = 2/3$ is given in Figure 5. In the limit $p_{0u} \to \infty$, then explicit expressions exist for the far-field and downstream parameters as given by (4.5), (4.6) and (4.14).

Finally, it remains to discuss the case $a_u = 0$. The limits $a_u \to 0^-$ with p_{0u} finite and $p_{0u} \to +\infty$ with $a_u = -1$ are equivalent as shown in [1]. Thus, following (4.5) and (4.6), we have explicit expressions for the parameters in terms of p_{0u} namely

$$C_{0u} = k_0(p_{0u})^{1-\frac{\alpha}{2}}, \quad d_{1u} = \kappa_1 p_{0u}^{\alpha-1}, \quad d_{2u} = \kappa_2 p_{0u}^{\alpha}, \quad d_{3u} = \kappa_3 p_{0u},$$

$$p_{0d} = p_{0u}, \quad C_{0d} = -C_{0u}, \quad d_{1d} = d_{1u}, \quad d_{2d} = -d_{2u}, \quad d_{3d} = d_{3u}, \quad a_d = k_d(p_{0u})^2. \tag{5.3}$$

The constants $k_0, \kappa_1, \kappa_2, \kappa_3$ are shown in Figure 3 for a range of α, whilst k_d is shown in Figure 5. We note that this case gives the largest value of a_d for a given value of p_{0u} i.e. the largest resultant shear rate at the downstream wall.

6. Discussion

This paper has used the natrual stress basis to complete the description of the local asymptotic solution for flow of UCM fluids around a re-entrant corner as a two parameter family. This is for each fixed re-entrant corner angle and assuming the absence of any separating streamlines so that the elastic fluid flows fully around the sharp corner. The two parameters used have been the upstream coefficients of the wall

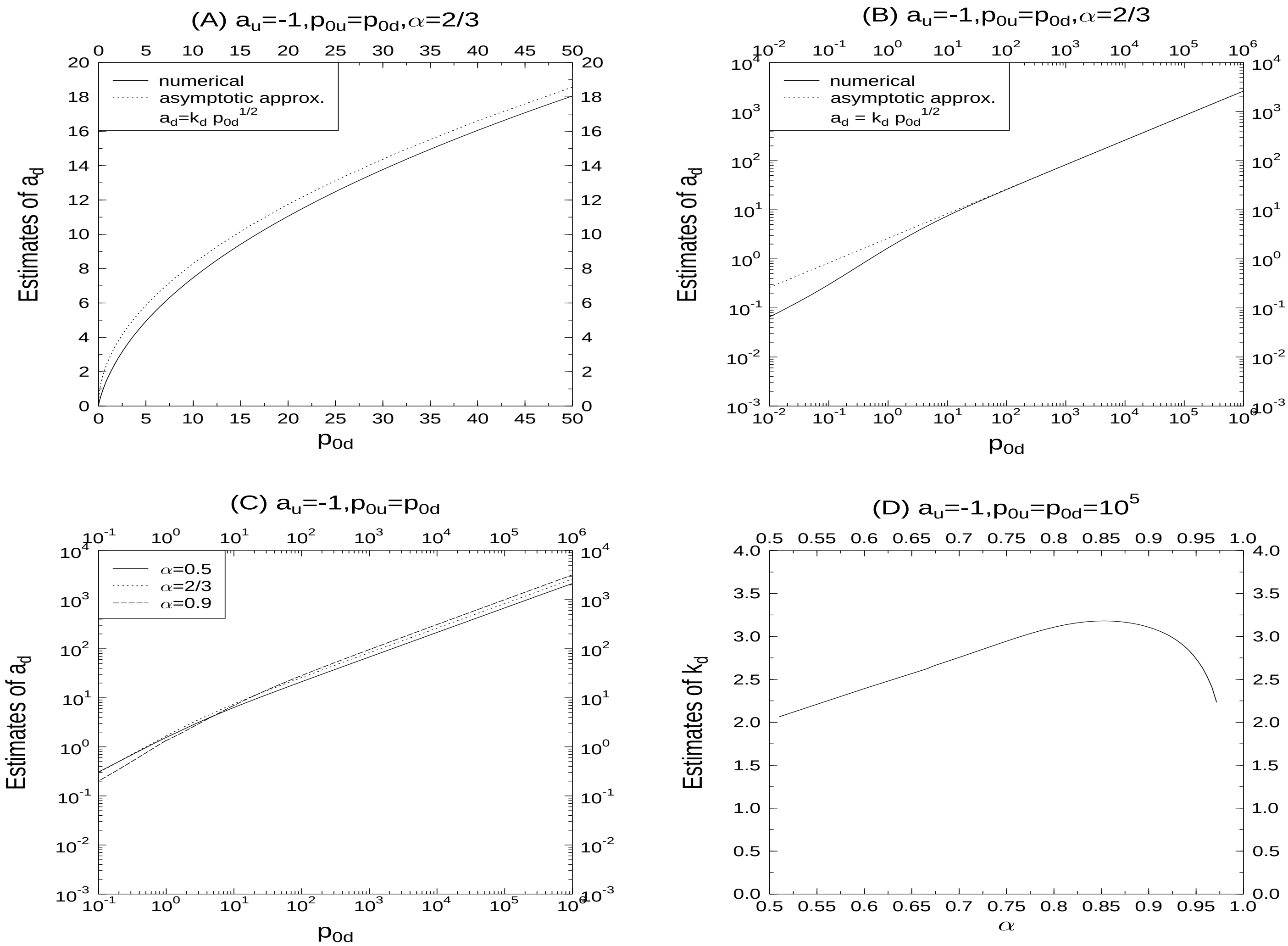

Figure 5: (A) and (B) show plots of the downstream values of a_d with $p_{0d} = p_{0u}$ in the case $a_u = -1, \alpha = 2/3$. The value of the function f'' at $\xi = \xi_0$ was used to estimate a_d. Also plotted for comparison is the analytical expression (4.14) using the estimate $k_d \approx 2.6219$ from the ratio a_d/p_{0d} at $p_{0d} = 10^5$. (C) shows estimates of a_d with p_{0d} for other selected α. (D) shows the variation of k_d with α for $a_u = -1$.

shear rate a_u and near wall pressure gradient p_{0u}. The natural stress basis allows determination of the appropriate information that is given to the downstream layer after being transmitted from the upstream layer through the core region. An important parameter for the downstream layer is the determination of the coefficient of the downstream wall shear rate a_d. In the case $\alpha = 2/3$, we have seen that $a_d > |a_u|$ for $p_{0u} > 0.5(a_u)^2$. For a given value of p_{0u} i.e. the upstream pressure gradient, the maximum value of the downstream wall shear rate is $k_d p_{0u}$ and occurs when the upstream wall shear rate is zero. This case has been commented upon by [3] as that which may be relevant when a separating streamline is present at the upstream wall.

It is clear that the natural stress basis is the appropriate formulation in which to address the re-entrant corner flow if a complete description of the parameteric solution is to be obtained. However, this parameteric solution description has benefited from being approached in both the Cartesian and natural stress formulations. Although the two approaches should be completely equivalent, arguably, the advantages of the Cartesian formulation relate to the initial determination of the scalings for the boundary layer as well as its subsequent analysis. The complete boundary layer analysis was performed in the first paper [1] in the Cartesian stress formulation, where the wall and far-field behaviours were determined to sufficient order and an eigenmode analysis used to determine the boundary count in the upstream and downstream cases. This analysis was repeated here in the natural stress basis formulation, showing consistency between the two formulations that was initially established in [1].

It is finally worth remarking on the type of singular perturbation problem given by the local asymptotic solution behaviour at the corner. It is apparent in this problem that there is only a partial (as oppose to complete) loss of the highest derivative terms in the governing equations in the outer region. The highest derivative terms we refer to are the upper convected stress derivative and rate-of-strain terms. Thus, although the upper convected stress derivative is maintained at leading order, there is loss of the rate-of-strain as well as relaxation terms, these latter terms being essential in order to recover viscometric stress behaviour at the walls. This retention of some (since only the rate-of-strain terms are dropped) of the highest derivatives in the outer region together with the hyperbolic nature of the equations implies that matching of the leading order inner (boundary layer) solution with the outer solution requires sufficiently high order terms in the outer solution. These inner regions at the walls have been aptly labelled by Renardy [6] as stress boundary layers. This should be contrasted with more traditional boundary layer problems where there is reduction in order of the governing equations in the outer region, with the highest derivatives being retained in a narrow region at the boundary. An example would be the case of high Reynolds number Newtonian fluid flow, where the inviscid flow or Euler equations are obtained away from boundaries and the viscous terms being recovered in narrow boundary layer regions.

References

[1] J.D. Evans, Re-entrant corner flows of UCM fluids: The Cartesian stress basis. *Submitted to J. Non-Newtonian Fluid Mech.* (2006).

[2] E.J. Hinch, The flow of an Oldroyd fluid around a sharp corner. *J. Non-Newtonian Fluid Mech.* **50** (1993), 161–171.

[3] J.M. Rallison and E.J. Hinch, The flow of an Oldroyd fluid past a reentrant corner: the downstream boundary layer. *J. Non-Newtonian Fluid Mech.* **116** (2004), 141–162.

[4] M. Renardy, How to integrate the upper convected Maxwell (UCM) stresses near a singularity (and maybe elsewhere,too). *J.Non-Newtonian Fluid Mech.* **52** (1994), 91–95.

[5] M. Renardy, A matched solution for corner flow of the upper convected Maxwell fluid. *J.Non-Newtonian Fluid Mech.* **58** (1995), 83–39.

[6] M. Renardy, High Weissenberg number boundary layers for the upper convected Maxwell fluid. *J. Non-Newtonian Fluid Mech.* **68** (1997), 125–132.

[7] M. Renardy, The high Weissenberg number limit of the UCM model and the Euler equations. *J. Non-Newtonian Fluid Mech.* **69** (1997), 293–301.

Appendix A. The wall expansion for $a > 0$

In the case $a > 0$, the wall expansion (3.20) contains exponentially small terms, which may be derived through a WKBJ analysis. We decompose the expansion into analytic and non-analytic parts as follows

$$\left(f(\xi), \tilde{\lambda}(\xi), \tilde{\mu}(\xi), \tilde{\nu}(\xi)\right) = \left(f_0(\xi), \tilde{\lambda}_0(\xi), \tilde{\mu}_0(\xi), \tilde{\nu}_0(\xi)\right) + \hat{\delta}\left(\hat{f}(\xi), \hat{\lambda}(\xi), \hat{\mu}(\xi), \hat{\nu}(\xi)\right), \text{ as } \xi \to 0 \tag{A.1}$$

where $f_0(\xi), \tilde{\lambda}_0(\xi), \tilde{\mu}_0(\xi), \tilde{\nu}_0(\xi)$ represent the regular power series expansion terms (the first few terms being recorded in (3.20)) and the terms with hats being transcendentally small. The small artificial gauge $\hat{\delta}$ has been introduced for convenience. Keeping terms of $O(\hat{\delta})$, the linearized equations satisfied by the hat variables are

$$\begin{aligned} 0 = \hat{\mu}' + \frac{2f_0''}{f_0'}\hat{\mu} + 2\left(\frac{\hat{f}''}{f_0'} - \frac{f_0''\hat{f}'}{(f_0')^2}\right)\mu_0 - \left(f_0'(1-f_0') + (3-\alpha)f_0 f_0''\right)\hat{\lambda} \\ - \left(\hat{f}'(1-2f_0') + (3-\alpha)(\hat{f}f_0'' + f_0\hat{f}'')\right)\lambda_0, \end{aligned} \tag{A.2}$$

$$(3-\alpha)(f_0\hat{\lambda}' + \hat{f}\tilde{\lambda}_0') + (2(2-\alpha)f_0' - 1)\hat{\lambda} + 2(2-\alpha)\hat{f}'\lambda_0 + 2\frac{f_0''}{f_0'^2}\hat{\mu} + 2\left(\frac{\hat{f}''}{f_0'^2} - 2\frac{f_0''\hat{f}'}{f_0'^3}\right)\mu_0 = 0, \tag{A.3}$$

$$(3-\alpha)(f_0\hat{\mu}' + \hat{f}\mu_0') + ((1-\alpha)f_0' - 1)\hat{\mu} + (1-\alpha)\hat{f}'\mu_0 + \frac{f_0''}{f_0'^2}\hat{\nu} + \left(\frac{\hat{f}''}{f_0'^2} - 2\frac{f_0''\hat{f}'}{f_0'^3}\right)\nu_0 = 0, \tag{A.4}$$

$$(3-\alpha)(f_0\hat{\nu}' + \hat{f}\nu_0') - (1+2f_0')\hat{\nu} - 2\hat{f}'\nu_0 + 2f_0'\hat{f}' = 0. \tag{A.5}$$

Assuming a WKBJ expansion for the hat variables, gives the two sets of possible behaviours

$$\left.\begin{aligned} &\hat{f} \sim K_1\xi^{q_1+5}\exp\left(-\tfrac{2}{a(3-\alpha)\xi}\right) \\ &\hat{\lambda} \sim -\frac{16K_1}{3(3-\alpha)^3a^4}\xi^{q_1-2}\exp\left(-\frac{2}{a(3-\alpha)\xi}\right) \\ &\hat{\mu} \sim -\frac{8K_1}{3(3-\alpha)^2a^2}\xi^{q_1+1}\exp\left(-\frac{2}{a(3-\alpha)\xi}\right) \\ &\hat{\nu} \sim -\frac{4K_1}{(3-\alpha)^2a}\xi^{q_1+3}\exp\left(-\frac{2}{a(3-\alpha)\xi}\right) \end{aligned}\right\}; \qquad \left.\begin{aligned} &\hat{f} = o\left(\xi^{q_2+6}\exp\left(-\tfrac{2}{a(3-\alpha)\xi}\right)\right) \\ &\hat{\lambda} \sim \frac{K_2}{a^2}\xi^{q_2-2}\exp\left(-\frac{2}{a(3-\alpha)\xi}\right) \\ &\hat{\mu} \sim \tfrac{1}{2}(3-\alpha)K_2\xi^{q_2+1}\exp\left(-\tfrac{2}{a(3-\alpha)\xi}\right) \\ &\hat{\nu} \sim \tfrac{1}{4}(3-\alpha)^2a^2K_2\xi^{q_2+4}\exp\left(-\tfrac{2}{a(3-\alpha)\xi}\right) \end{aligned}\right\}; \tag{A.6}$$

where

$$q_1 = \frac{(1+\alpha)}{(3-\alpha)} - \frac{2b}{3(3-\alpha)a^2}, \qquad q_2 = -4\frac{(2-\alpha)}{(3-\alpha)} - \frac{2b}{3(3-\alpha)a^2}, \tag{A.7}$$

and K_1, K_2 being arbitrary constants. These could alternatively be deduced using (3.19) and the exponentially small terms obtained in the Cartesian formulation (see section 3.3 in [1]).

Consequently, we have the wall expansion

as $\xi \to 0$
$$f(\xi) = \frac{1}{2}a\xi^2 + \frac{1}{3!}b\xi^3 + \ldots + \exp\left(-\frac{2}{a(3-\alpha)\xi}\right)\left[K_1\xi^{q_1+5}\left(1+O(\xi)\right) + o\left(K_2\xi^{q_2+6}\right)\right],$$
$$\tilde{\lambda}(\xi) = 2\xi^{-2} + \frac{2}{a}(b+3(1-\alpha)a^2)\xi^{-1} + \ldots$$
$$+\exp\left(-\frac{2}{a(3-\alpha)\xi}\right)\left[-\frac{16K_1}{3(3-\alpha)^3a^4}\xi^{q_1-2}\left(1+O(\xi)\right) + \frac{K_2}{a^2}\xi^{q_2-2}\left(1+O(\xi)\right)\right],$$
$$\tilde{\mu}(\xi) = a + (b+2(1-\alpha)a^2)\xi + \ldots,$$
$$+\exp\left(-\frac{2}{a(3-\alpha)\xi}\right)\left[-\frac{8K_1}{3(3-\alpha)^2a^2}\xi^{q_1+1}\left(1+O(\xi)\right) + \frac{1}{2}(3-\alpha)K_2\xi^{q_2+1}(1+O(\xi))\right],$$
$$\tilde{\nu}(\xi) = a^2\xi^2 + a(b+(1-\alpha)a^2)\xi^3 + \ldots$$
$$+\exp\left(-\frac{2}{a(3-\alpha)\xi}\right)\left[-\frac{4K_1}{(3-\alpha)^2a}\xi^{q_1+3}(1+O(\xi)) + \frac{1}{4}(3-\alpha)^2a^2K_2\xi^{q_2+4}(1+O(\xi))\right].$$

Appendix B. The far-field behaviour eigenmodes

Writing

$$f \sim C_0\xi^{3-\alpha}(1+\hat{\delta}\hat{f}(\xi)), \quad \tilde{\lambda} \sim d_1\xi^{-4+2\alpha}(1+\hat{\delta}\hat{\lambda}(\xi)), \quad \tilde{\mu} \sim d_2\xi^{-1+\alpha}(1+\hat{\delta}\hat{\mu}(\xi)), \quad \tilde{\nu} \sim d_3\xi^2(1+\hat{\delta}\hat{\nu}(\xi)), \tag{B.1}$$

with $\hat{\delta}$ a small artificial gauge, we linearize about the far-field behaviour by keeping terms of $O(\hat{\delta})$ in (3.12)–(3.15). Further, keeping only the leading order terms of the resulting linearized equations, we obtain the simplified fifth order system

$$\xi^2\hat{f}'' + 2(2-\alpha)\xi\hat{f}' + (1-\alpha)(3-\alpha)(2\hat{f}+\hat{\lambda}),$$
$$(3-\alpha)\hat{\lambda}' + 2(2-\alpha)\hat{f}' = 0, \qquad (3-\alpha)\hat{\mu}' + (1-\alpha)\hat{f}' = 0, \qquad (3-\alpha)\hat{\nu}' - 2\hat{f}' = 0.$$

These linear homogeneous equations give the eigenmodes as

$$\left.\begin{array}{l}\hat{f}=1\\ \hat{\lambda}=-2\\ \hat{\mu}=0\\ \hat{\nu}=0\end{array}\right\};\quad \left.\begin{array}{l}\hat{f}=0\\ \hat{\lambda}=0\\ \hat{\mu}=1\\ \hat{\nu}=0\end{array}\right\};\quad \left.\begin{array}{l}\hat{f}=0\\ \hat{\lambda}=0\\ \hat{\mu}=0\\ \hat{\nu}=1\end{array}\right\};\quad \left.\begin{array}{l}\hat{f}=\xi^{-2+2\alpha}\\ \hat{\lambda}=-\frac{2(2-\alpha)}{(3-\alpha)}\xi^{-2+2\alpha}\\ \hat{\mu}=-\frac{(1-\alpha)}{(3-\alpha)}\xi^{-2+2\alpha}\\ \hat{\nu}=\frac{2}{(3-\alpha)}\xi^{-2+2\alpha}\end{array}\right\};\quad \left.\begin{array}{l}\hat{f}=\xi^{-1}\\ \hat{\lambda}=-\frac{2(2-\alpha)}{(3-\alpha)}\xi^{-1}\\ \hat{\mu}=-\frac{(1-\alpha)}{(3-\alpha)}\xi^{-1}\\ \hat{\nu}=\frac{2}{(3-\alpha)}\xi^{-1}\end{array}\right\}; \tag{B.2}$$

corresponding to the linearly independent solutions. The first three eigenmodes correspond to small changes in the parameters C_0, d_2, d_3, whilst the last two modes are associated with higher order terms in the far-field expansion. Specifically, the first mode emphasizes that d_1 is linked to C_0 (see the first expression in (3.22)), whilst the second mode and third modes show that this is not the case for d_2 and d_3. In fact, in [1] we showed in the Cartesian formulation that d_2 and d_3 contained two additional free parameters which we called C_4 and C_5, the expressions in (3.22) are for the particular case $C_4 = 0$. The fourth and fifth modes are associated with the parameters C_2, C_3 of the Cartesian stress formulation.